High Energy Physics and Nuclear Physics

Volume 16, Number 2

Evolution of Heavy Ion Reaction Mechanism in the Energy Region from 10 to 100 MeV/A

Zhu Quanling[1], Ge Lingxiao[1] and Li Zhuxia[2]

[1]Institute of Modern Physics, the Chinese Academy of Sciences, Lanzhou, Gansu, China
[2]Institute of Atomic Energy, Beijing, China

The dynamical process of the heavy ion collision in the energy region from 10 to 100 MeV/A is investigated by the quantum molecular dynamics model. According to the calculated mass distribution, the evolution of the mass and density distribution with respect to time is calculated. The reaction mechanism and its characteristics are predicted and compared with those obtained from the BUU model.

1. INTRODUCTION

During last 10 years, our knowledge about the heavy ion collision (HIC) in the energy region from the Coulomb barrier up to 150 MeV/A has been enhanced considerably by the investigations carried out on the facilities such as CERN-SC, GANIL, MSU, RIKEN and HIRFL. Both experimental and theoretical studies show that in this region, the mean field effect, two-body interaction and pauli blocking effect dominate the collision. Several microscopic models have been developed to describe HIC. So far, the BUU or VUU theory has been applied successfully to describe the dynamic process [1]. But similar to TDHF, the BUU equation is a one-body density matrix equation where the many-body correlations [2] are not sufficiently considered. In the numerical method (test particle method) employed to solve BUU equation, an ensemble average is imposed to calculate the smooth single particle distribution function. Thus the density fluctuations is smeared and a continued low density region is formed. As a consequence, the fragment formation and the fragmentation cannot be described.

Recently, based on the classical molecular dynamics (CMD) model, the quantum molecular dynamics model, which has great advantages in the studies on the fragment formation and the fragmentation, has been proposed [3]. In this model, each nucleon is represented by a double

Supported by the National Natural Science Foundation of China.
Received on June 13, 1991.

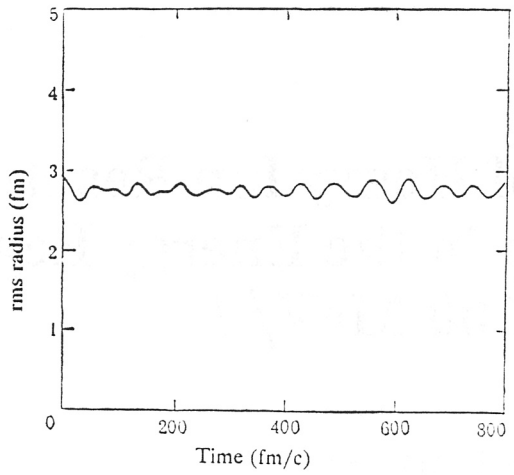

Fig. 1
The evolution of the root mean square radius of ^{40}Ca nuclei with respect to time.

Gaussian wave packet and, instead of the mean field, the interactions among wave packets are caused by the two-body and three-body interactions of the Skyrme type. In contrast with BUU calculations, where hundreds of simulations for one reaction event were performed, the simulation is carried out from one event to another. Thus, the fluctuations and n-body correlations remain. Now the theoretical foundation of QMD is still under research [4]. In addition, the BUU theory with fluctuations and many-body correlations has also been proposed [5].

The reaction dynamic properties of HIC described by the QMD model at the higher incident energy (1.05 GeV/A) have been studied extensively [3]. Recently, this model is extended into the lower energy region to study the fusion reaction [6]. In this paper, by using the QMD model, the evolution of the reaction mechanism with respect to the incident energy from 10 and 100 MeV/A and various impact parameters in the ^{40}Ca + ^{40}Ca system are explored. The mass distribution, evolution of mass distribution and density distribution with respect to time in the reaction plane is calculated and analyzed at different incident energies and impact parameters. In the central collision, it has been predicted both theoretically and experimentally that the reaction mechanism tends to transit from complete fusion (CF) to incomplete fusion (ICF), finally to fragmentation (FRAG) when the incident energy increases from 10 to 100 MeV/A. However, in the peripheral collision less knowledge has been obtained because it is difficult to distinguish reaction mechanisms in the experiment. By analyzing the evolution of mass distribution at different energies, it is found that the reaction mechanism does not transit sharply, but develops continuously, and different mechanisms may coexist and compete with each other at 50 MeV/A. In the case of the peripheral collision, as the incident energy increases, according to the criteria mentioned for the mass distribution of the deep inelastic collision (DIC) and participant-spectator (P-S), the reaction mechanism may change from CF or DIC to P-S and finally to FRAG.

2. QMD MODEL

We assume that each nucleon is represented by a double Gaussian wave packet in the phase space. The Wigner distribution function $f(r, p, t)$ for the total system is given by [7]

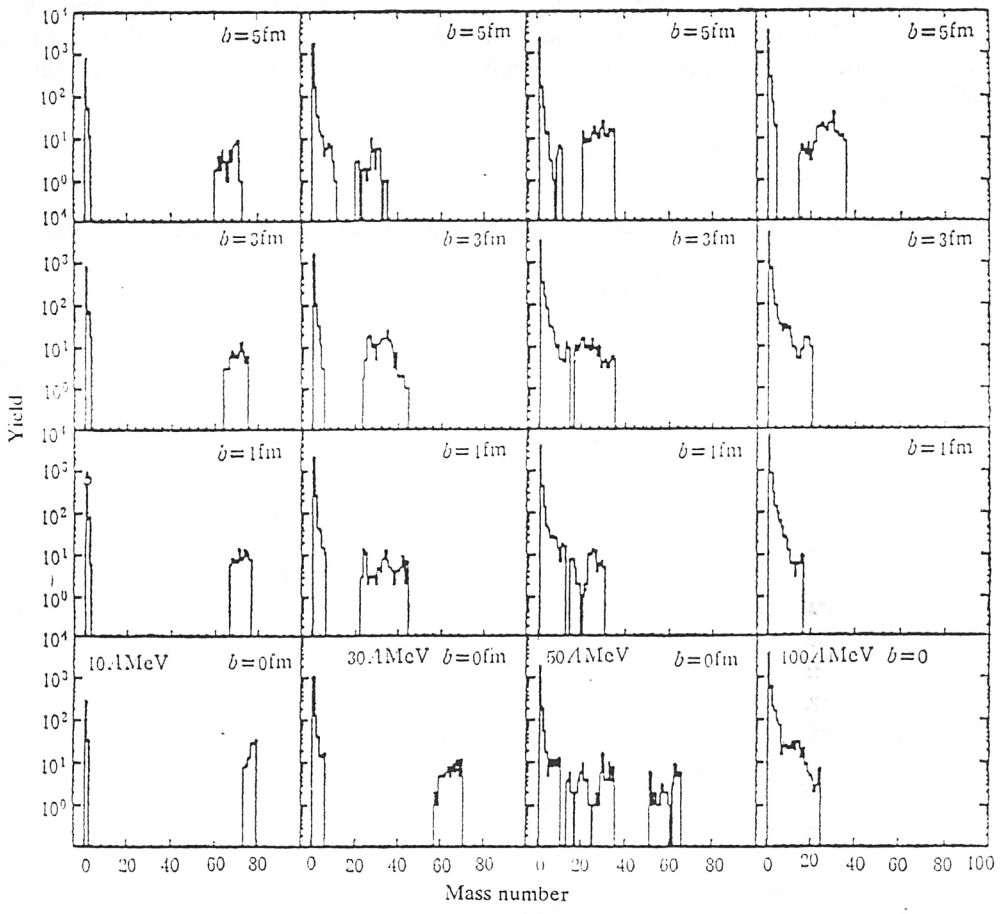

Fig. 2
The mass distribution at different energies and parameters in the reaction $^{40}Ca + {}^{40}Ca$.

$$f(\boldsymbol{r}, \boldsymbol{p}, t) = \sum_i f_i(\boldsymbol{r}, \boldsymbol{p}, t) = \sum_i \frac{1}{(\pi\hbar)^3} \exp\{-(\boldsymbol{r} - \boldsymbol{r}_i)^2/2L - (\boldsymbol{p} - \boldsymbol{p}_i)^2 \cdot 2L/\hbar^2\}, \quad (1)$$

where the distribution width L in the coordinate space keeps constant value ($L = 2.0$ fm^2) all the time, namely the wave function is not dispersed. The value of L is chosen in such a way that L is neither too large to acquire a satisfactory nuclear surface, nor too small to obtain the reasonable momentum due to the limitation of the uncertainty relation. According to Eq.(1), the density in the coordinate space is given by

$$\rho(\boldsymbol{r}, t) = \sum_i \frac{1}{(2\pi L)^{3/2}} \exp\{-(\boldsymbol{r} - \boldsymbol{r}_i)^2/2L\}, \quad (2)$$

The normalization condition is written as

$$\iint f(\boldsymbol{r}, \boldsymbol{p}, t) d\boldsymbol{r} d\boldsymbol{p} = A, \quad (3)$$

where A represents the mass number of the nucleus. The interaction between nucleons can be obtained via two- and three-body interactions where the short range potential of the Skyrme type and long range interaction of the Yukawa and Coulomb types are used. The total energy for particle i can be written as

$$H_i = T_i + \frac{1}{2}\sum_{i(j\neq i)} U_{ij}^{(2)} + \frac{1}{3}\sum_{j,k(j\neq k, j,k\neq i)} U_{ijk}^{(3)}. \tag{4}$$

where the two-body and three-body interactions are obtained from the following equations:

$$U_{ij}^{(2)} = \int f_i(\boldsymbol{r},\boldsymbol{p},t)\cdot f_i(\boldsymbol{r}',\boldsymbol{p}',t)V^{(2)}(\boldsymbol{r}-\boldsymbol{r}')\mathrm{d}\boldsymbol{r}\mathrm{d}\boldsymbol{p}\mathrm{d}\boldsymbol{r}'\mathrm{d}\boldsymbol{p}', \tag{5.1}$$

$$U_{ijk}^{(3)} = \int f_i(\boldsymbol{r},\boldsymbol{p},t)\cdot f_j(\boldsymbol{r}',\boldsymbol{p}',t)\cdot f_k(\boldsymbol{r}'',\boldsymbol{p}'',t)V^{(3)}(\boldsymbol{r},\boldsymbol{r}',\boldsymbol{r}'')\mathrm{d}\boldsymbol{r}\mathrm{d}\boldsymbol{p}\mathrm{d}\boldsymbol{r}'\mathrm{d}\boldsymbol{p}'\mathrm{d}\boldsymbol{r}''\mathrm{d}\boldsymbol{p}'', \tag{5.2}$$

where

$$V^{\mathrm{tot}} = V^{(2)} + V^{(3)} = V^{\mathrm{loc}} + V^{\mathrm{Yuk}} + V^{\mathrm{Coul}}, \tag{6.1}$$

$$V^{\mathrm{loc}} = t_1\delta(\boldsymbol{r}-\boldsymbol{r}') + t_2\delta(\boldsymbol{r}-\boldsymbol{r}')\cdot\delta(\boldsymbol{r}-\boldsymbol{r}''), \tag{6.2}$$

$$V^{\mathrm{Yuk}} = V_{\mathrm{Y}}\cdot\exp\{-\gamma\cdot|\boldsymbol{r}-\boldsymbol{r}'|\}/|\boldsymbol{r}-\boldsymbol{r}'|, \tag{6.3}$$

$$V^{\mathrm{Coul}} = V_{\mathrm{C}}\cdot\frac{1}{|\boldsymbol{r}-\boldsymbol{r}'|}. \tag{6.4}$$

The potential felt by the i-th nucleon can be obtained

$$U_{\mathrm{loc}}^{(2)} = t_1\sum_{j(j\neq i)}\frac{1}{(4\pi L)^{3/2}}\exp\{-(\boldsymbol{r}_i-\boldsymbol{r}_j)^2/4L\}, \tag{7.1}$$

$$U_{\mathrm{loc}}^{(3)} = t_2\sum_{j(j\neq i)}\frac{1}{(4\pi L)^{3/2}}\exp\{-(\boldsymbol{r}_i-\boldsymbol{r}_j)^2/4L\}\Big(\sum_{k(k\neq i,j)}\frac{1}{(4\pi L)^{3/2}}\exp\{-(\boldsymbol{r}_i-\boldsymbol{r}_k)^2/4L\}\Big), \tag{7.2}$$

$$U_{\mathrm{Coul}}^{(2)} = V_{\mathrm{C}}\sum_{j(j\neq i)}\frac{1}{r_{ij}}\,\mathrm{erf}\left(\frac{r_{ij}}{\sqrt{4L}}\right), \tag{7.3}$$

$$U_{\mathrm{Yuk}}^{(2)} = \frac{1}{2}V_{\mathrm{Y}}\sum_{j(j\neq i)}\frac{1}{r_{ij}}\cdot\exp\{L\gamma^2\}\Big[\exp\{-\gamma r_{ij}\}\cdot\mathrm{erfc}\left(\sqrt{L}\,\gamma-\frac{r_{ij}}{\sqrt{4L}}\right) - \exp\{\gamma r_{ij}\}\,\mathrm{erfc}\left(\sqrt{L}\,\gamma+\frac{r_{ij}}{\sqrt{4L}}\right)\Big], \tag{7.4}$$

where $r_{ij} = |\boldsymbol{r}_i - \boldsymbol{r}_j|$, and $\mathrm{erf}(x)$ and $\mathrm{erfc}(x)$ are the error function and remnant error function, respectively. The coefficients in the above equations are determined by fitting the ground state properties of the nucleus. They are $t_1 = -124/\rho_0$ MeV, $t_2 = 70.5/\rho_0^2$ MeV ($\rho_0 = 0.16$ fm^{-3}), $V_{\mathrm{C}} = (Z/A)^2\cdot e^2$ (Z and A are the charge number and mass number of the nucleus, respectively), $V_{\mathrm{Y}} = -7$ MeV, and $\gamma = 0.8$ fm^{-1}. As a result, similar to the BUU calculation [8], the stiff equation of state ($K = 380$ MeV) is obtained.

In the phase space of the ground state, the central positions and central momenta of wave packets are distributed randomly within the global regions whose radii are $R = 1.142A^{1/3}$ and the

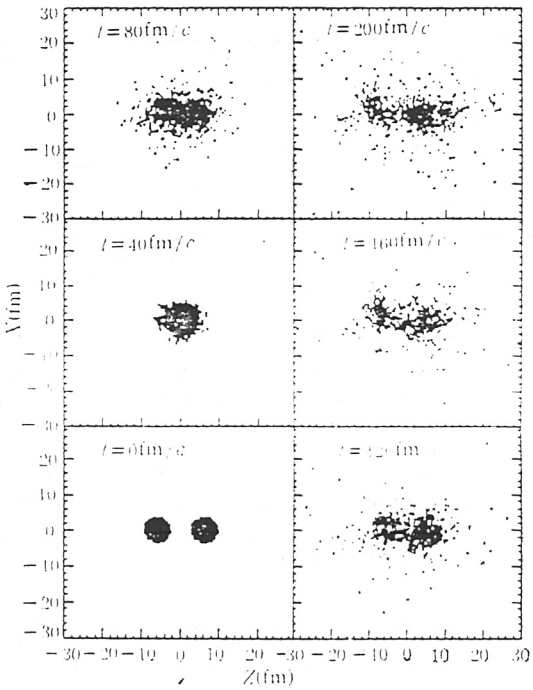

Fig. 3
The development of the density distribution with respect to time in the collision ^{40}Ca + ^{40}Ca at 50 MeV/A and b = 0 fm.

Fermi momentum P_F, respectively. In the coordinate space, the distance between the centers of two wave packets should have a value larger than 1.7 fm. The central coordinate and momentum of each wave packet must obey the uncertainty relation. After initialization, the central position and momentum of the Gaussian wave packet propagate in terms of Hamilton's equations

$$\dot{\boldsymbol{p}}_i = -\frac{\partial H_i}{\partial \boldsymbol{r}_i}, \tag{8.1}$$

$$\dot{\boldsymbol{r}}_i = \frac{\partial H_i}{\partial \boldsymbol{p}_i}. \tag{8.2}$$

Similar to the BUU method, we assume that the collision between two wave packets is independent.

3. EVOLUTION OF REACTION MECHANISM WITH RESPECT TO INCIDENT ENERGY AND IMPACT PARAMETERS

In contrast to the BUU theory, the QMD model is favorable to the study of the fragment formation because it remains incorporated fluctuations and correlations. Meanwhile, by using the distribution function of Gaussian type, it is also easy to calculate surface and Coulomb energies and to change the calculation in the nuclear matter into that in the finite nuclei. The criterion for the fragment formation is the same as that in Ref. [9]. If the distance between two nucleons is smaller

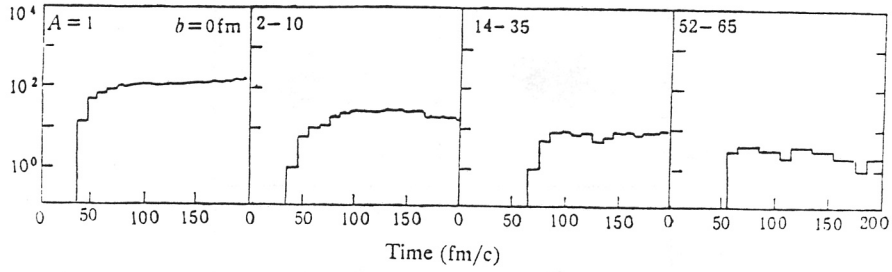

Fig. 4
The evolution of different mass distribution with respect to time in the reaction $^{40}Ca + {}^{40}Ca$ at 50 MeV/A and b = 0 fm.

than the critical value d_{Crit}, e.g., d_{Crit} = 3 fm, these two nucleons are considered in the same cluster. By repeating this judgement for all nucleons, we can divide the system into several nucleons and clusters. Our numerical calculations indicate that the mass distribution is not very sensitive to the value of d_{Crit}, for instance, 3.0 fm, 4.0 fm or 5.0 fm. Moreover, in our calculations, we do not put the special cut off in the momentum space.

In order to extend the QMD into the lower energy region, the stability condition of the ground state propagation is checked carefully. The evolution of root mean square (rms) radius with respect

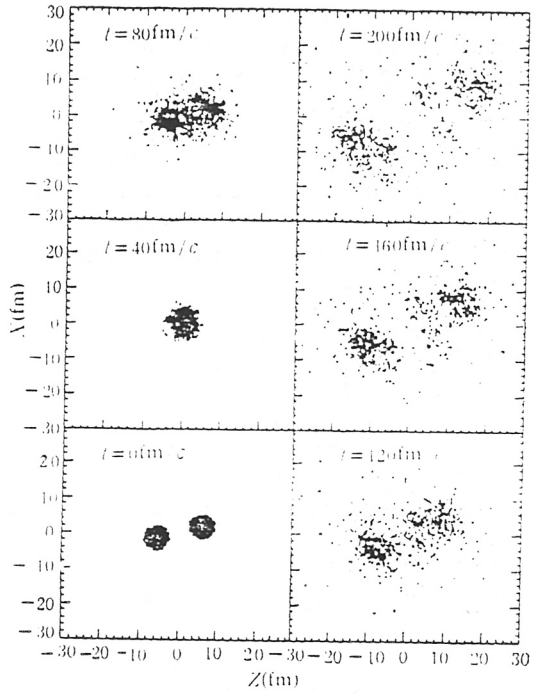

Fig. 5
The development of the density distribution with respect to time in the collision $^{40}Ca + 4^{0}Ca$ at 50 MeV/A and b = 3 fm.

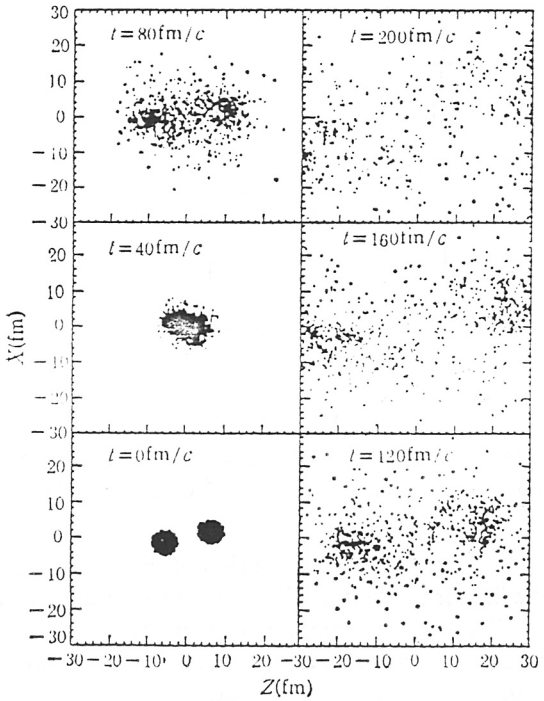

Fig. 6
The evolution of the density distribution with respect to time in the reaction ^{40}Ca + ^{40}Ca at 50 MeV/A and b = 5 fm.

to time for ^{40}Ca in the ground state is shown in Fig. 1. Obviously, the rms radius remains almost constant with a small fluctuation of 800 fm/c.

The calculated mass distribution at different energies (such as 10, 30, 50, 100 MeV/A) and different impact parameters (such as 0, 1, 3, 5 fm) in the ^{40}Ca + ^{40}Ca system are shown in Fig. 2, where the mass yield is obtained from the ten-event simulation.

3.1 Head-on Collisions

Fig. 2 shows that when b = 0 fm, the mass distribution of fragments at 10 MeV/A is one heavy fragment and a few nucleons. As the incident energy increases (e.g. 30 MeV/A), the masses of heavy fragments become smaller and the number of nucleons and smaller clusters increase. This means that the reaction mechanism changes from CF to ICF. The linear momentum transfer (LMT) is about 75% at 30 MeV/A and 95% at 10 MeV/A. This has also been obtained in the BUU calculation [1] and Ref. [6]. As the bombarding energy increases to 50 MeV/A, the mass distribution is very complex. There are bigger clusters with A about 60 and intermediate mass fragments (IMF) with A about 20 which connect the area of fragments of A < 40. The heavier clusters originate from the process of ICF, while the IMF comes from the mechanism of FRAG and P-S. This means that the reaction mechanisms coexist and compete with each other. When the incident energy increases up to 100 MeV/A, the head-on collision causes the complete explosion (CE). Meanwhile, the evolution of the reaction mechanism can also be seen intuitively from the evolution of the density distribution with respect to time in the x-z plane. We show the evolution of the density distribution

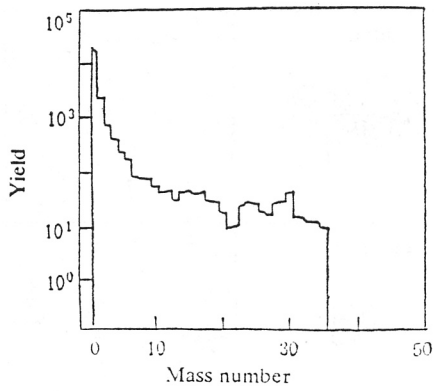

Fig. 7
The mass distribution with parameters b = 0, 1, 3 and 5 fm, respectively, in the reaction at ^{40}Ca + ^{40}Ca at 100 MeV/A.

in the x-z plane at 50 MeV/A in Fig. 3 and the evolution of different mass distribution in Fig. 4. From Fig. 4, we find that all the lighter clusters, IMF and the heavier clusters appear in the head-on collision process at 50 MeV/A. Thus, the reaction mechanism does not transit sharply, but develops continuously. The fact that different reaction mechanisms may coexist and compete at 50 MeV/A causes difficulties in the experimental and theoretical studies.

3.2 Nearly Central and Peripheral Collisions

From the theoretical and experimental studies on the low energy HIC, we know that the fusion cross section is the main portion of the total reaction cross section and the fusion takes place under many impact parameters. From Fig. 2, we find that at 10 MeV/A and b = 0-5 fm, the mass distribution is composed of one heavy fragment and a small amount of nucleons and smaller clusters. However, as the impact parameter increases, the probability of fusion becomes obviously smaller, the width of heavier fragments distribution becomes wider and the distribution moves towards the lighter mass number region. We do not calculate the mass distribution under the larger impact parameter because the mechanisms in this case are DIC and quasi-elastic scattering (QES).

When the incident energy increases up to 30 MeV/A, the mass distribution becomes one heavy cluster and the mass number is slightly less than the mass numbers of the projectile and target plus some nucleons and smaller clusters, and less IMF. In comparison with the DIC at the lower energy, we call this a DIC-like component. As is known, for DIC at the lower energy, there is mass distribution around the mass numbers of the projectile and target. Its peak is located at the place very close to the masses of the projectile and target, and its width becomes gradually wider when the total kinetic energy is lost (the impact parameter decreases). When the incident energy becomes higher (e.g., 30 MeV/A), because of the emission of preequilibrium particles and increase of lighter clusters, the center of the mass distribution moves to the region where the mass is lighter than the masses of the projectile and target. Meanwhile, there still exist the fragments whose mass is larger than those of the projectile and target, because the nucleons are exchanged between the target and projectile. This is a very important difference between DIC and P-S. When the impact parameter decreases, we further find the relaxation process. To distinguish from the low energy DIC, we call this mechanism IDIC.

Table 1
The reaction mechanism evolves with the incident energy and impact parameter.

Impact parameter \ Energy (MeV/A) Reaction mechanism	10	30	50	100
5	CF	IDIC	P-S	P-S
3	CF	IDIC	P-S	P.T. Frag.
1	CF	IDIC	P-S	TE
0	CF	IDIC	ICF	TE

When the incident energy goes up to 50 MeV/A, the fragments whose mass is larger than that of the projectile and target no longer exist and IMF increase obviously. This is just the P-S picture. We can clearly see the participant and spectators of the projectile and target in Fig. 5, where the density distribution as a function of time in the x-z reaction plane is plotted. As the impact parameter decreases, the probability of IMF increases gradually. In the smaller impact parameter case, the mass of spectators of the projectile and target becomes smaller because in the participant region more nucleons are produced. Therefore, the heaviest residues of the projectile and target at b = 1 fm are smaller than that at b = 3 fm and b = 5 fm (Fig. 2).

When the incident energy is 100 MeV/A and b = 5 fm (Fig. 2), the reaction mechanism seems to be the P-S picture. According to Fig. 6, the mechanism is the fragmentation of projectile and target. In the central collision, no heavy clusters survives, but the cluster with $5 < A < 24$ does. In the peripheral reaction, the remnants of the projectile and target are in the region of $A < 35$. In comparison with the QMD calculation for the ^{197}Au + ^{197}Au system at 1.05 GeV/A [4], we do not find the emission pattern of the sideward flow at 100 MeV/A. We plot the mass distribution contributed by four impact parameters in Fig. 7. From this figure, we find that at the central collision, this distribution approaches the power law. However, the general tendency of the mass yield distribution does not agree with the prediction of the power-law from the liquid-gas phase transition.

4. SUMMARY AND DISCUSSION

The reaction mechanism and characteristics of HIC are predicted according to the mass distribution and the evolution of the mass and density distribution with respect to time in the QMD framework. In comparison with the BUU theory, QMD is more complete and clearer, especially in the transition energy region where the reaction mechanism is very complex. Therefore, QMD is essential in describing the reaction dynamics properly. The calculated results are summarized in Table 1.

Thus, we conclude:

1) The reaction mechanisms do not transit sharply, but develop continuously. The different reaction mechanisms may coexist and compete at 50 MeV/A. In the case of the central collision, the reaction mechanism evolves from CF to ICF, and finally to fragmentation.

2) The reaction mechanism is very complex in the nearly central and peripheral collisions. According to our criteria for the mass distribution of DIC and P-S, the reaction mechanism evolves from CF or DIC to IDIC then P-S and finally to fragmentation.

3) When the incident energy increases, the component of ICF reduces and disappears eventually. Except for the preequilibrium particle emission [10], the possible reason is that only a few

impact parameter cases contribute to ICF. Finally, the QMD model should be further improved. In the case of the light system, the dispersion range of the density distribution in space is larger than usual, and some calculated results depend sensitively on different simulations. The study of DIC and IDIC at the lower energy region is underway.

REFERENCES

[1] Zhang Fengshou and Ge Lingxiao, *High Energy Phys. and Nucl. Phys.* (in Chinese), **14** (1990), p. 561.
[2] Ge Lingxiao and Zhuo Yizhong, *High Energy Phys. and Nucl. Phys.* (in Chinese), **13** (1989), p. 652.
[3] Aichelin, J. *et al.*, *Phys. Rev.*, **C37** (1988), p. 2451.
[4] Aichelin, J., "Quantum" Molecular Dynamics a dynamical microscopic N-body approach to investigate fragment formation and the nuclear equation of state in heavy ion collisions, to be published.
[5] Randrup, J., and Remaud, B., *Nucl. Phys.*, **A514** (1990), p. 339.
[6] Maruyama, T., Ohnishi, A., and Horiuchi, *Phys. Rev.*, **C42** (1990), p. 386.
[7] Carruthers, P., and Zachariasen, M., *Rev. Mod. Phys.*, **55** (1983), p. 245.
[8] Bertch, G. F. *et al.*, *Phys. Rep.*, **160** (1988), p. 189.
[9] Hartnack, C. *et al.*, *Nucl Phys.*, **A495** (1989), p. 303.
[10] Ge Lingxiao and Zhang Fengshou, *Chin. J. Nucl. Phys.*, **12** (1990), p. 207.